Covalent immobilisation of magnetic nanoparticles on surfaces via strain---promoted azide---alkyne click chemistry

Raluca M. Fratila,*[a,b] Marcos Navascuez,[a] Javier Idiago-López,[a] Maite Eceiza,[c] José Ignacio Miranda,[c] Jesús M. Aizpurua,[c] and Jesús M. de la Fuente*[a,b,d]

Herein we report the synthesis of "clickable" magnetic nanoparticles (MNPs) stable in suspension in physiological media for bioorthogonal click chemistry applications. The MNPs incorporate in their coating a cyclooctynyl derivative for strain-promoted azide-alkyne (SPAAC) cycloaddition and either a polyethylene glycol or a glucose moiety to ensure MNP stability in physiological media. Their reactivity towards azide-functionalised Si surfaces was investigated, demonstrating their potential as bioorthogonal probes.

The term "click chemistry", coined in 2001 by K. B. Sharpless, includes a series of chemical reactions having unique features in terms of selectivity, rapid kinetics, simplicity, lack of side products, robustness and efficiency.[1] The copper-catalysed 1,3-dipolar cycloaddition between azides and terminal alkynes (CuAAC),[2,3] arguably the typical example of "click" reaction, has been extensively employed for a wide range of applications in organic, bioorganic and medicinal chemistry, polymer, surface and materials science.[4–7] However, its widespread use in biology is hampered by the cytotoxicity of the copper ion.[8] To circumvent this problem, Bertozzi and co-workers developed a copper-free alternative using cyclic alkynes instead of linear ones (Scheme 1). The ≈ 18 kcal · mol^{-1} ring strain of the cyclic alkyne is released in the transition state of the reaction resulting in fast reaction kinetics at room temperature and eliminating the need for the Cu(I) catalyst, hence the name "strain-promoted" click azide-alkyne cycloaddition (SPAAC).[9] This copper-free version belongs to the family of bioorthogonal click chemistry reactions[10,11] in which the azide partner is typically installed on cell surface glycans by metabolic transformation of unnatural azido-sugars.[12]

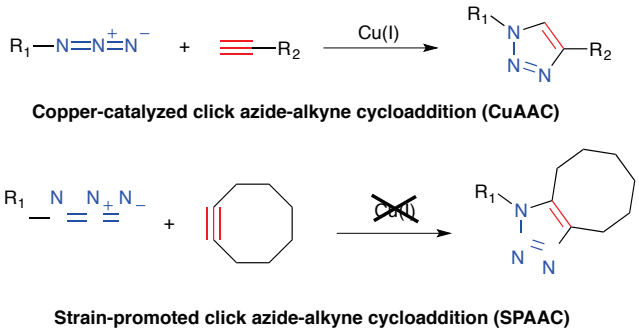

Scheme 1 Strain-promoted "click" azide-alkyne cycloaddition

Since 2004, the SPAAC reaction has been used to selectively label cell surface proteins,[13] investigate protein-protein interactions,[14] analyse glycoproteins on cell surfaces,[15] assess spatiotemporal changes in glycan expression during zebrafish embryo development[16] and perform *in vivo* imaging of glycan trafficking in *C. elegans* nematode[17] and mice.[18] The copper-free alkyne-azide cycloaddition has been also explored for model cell membrane derivatisation.[19] However, its use in nano(bio)technology remains relatively little exploited so far. In this sense, the first examples of SPAAC applied to nanotechnology were the bioderivatisation of polymeric nanoparticles[20] and quantum dots[21] with cyclooctynes. Kim and co-workers also reported the use of bioorthogonal click chemistry for tumour-targeted delivery of liposomes and chitosan nanoparticles (NPs) functionalised with strained alkynes.[22,23] In a different approach, mesoporous silica NPs bearing a dibenzocyclooctyne (DBCO) functionality were used for *in vivo* positron emission tomography (PET) imaging of subcutaneous tumours in mice pre-treated with an ^{18}F-azide radiotracer.[24] Gobbo *et al.* introduced the concept of interfacial SPAAC for the preparation of hybrid nanomaterials and illustrated the versatility of the approach by synthesising both azide- and DBCO-modified gold NPs for linking with

[a] *Institute of Materials Science of Aragón (ICMA – CSIC/University of Zaragoza) C/ Pedro Cerbuna 12, 50009, Zaragoza, Spain. E-mail: rfratila@unizar.es*
[b] *Centro de Investigación Biomédica en red en Bioingenieria Biomateriales y Nanomedicina (CIBER-BBN), Zaragoza, Spain*
[c] *José Mari Korta R&D Center, Basque Country University, UPV/EHU, P.O. 20018, Donostia-San Sebastián, Spain.*
[d] *Institute of Nano Biomedicine and Engineering, Department of Instrument Science and Engineering, Shanghai Engineering Centre for Intelligent Diagnosis and Treatment Instrument. Shanghai Jiao Tong University, Dongchuan Road 800, 200240, Shanghai, PR of China. E-mail: jmfuente@unizar.es*
Electronic Supplementary Information (ESI) available: details on the synthesis and characterisation of the MNPs and molecules **3**-**4** as well as MNP immobilisation on surfaces. See DOI: 10.1039/x0xx00000x

DBCO-functionalised carbon nanotubes and azide-decorated polymersomes, respectively.[25,26]

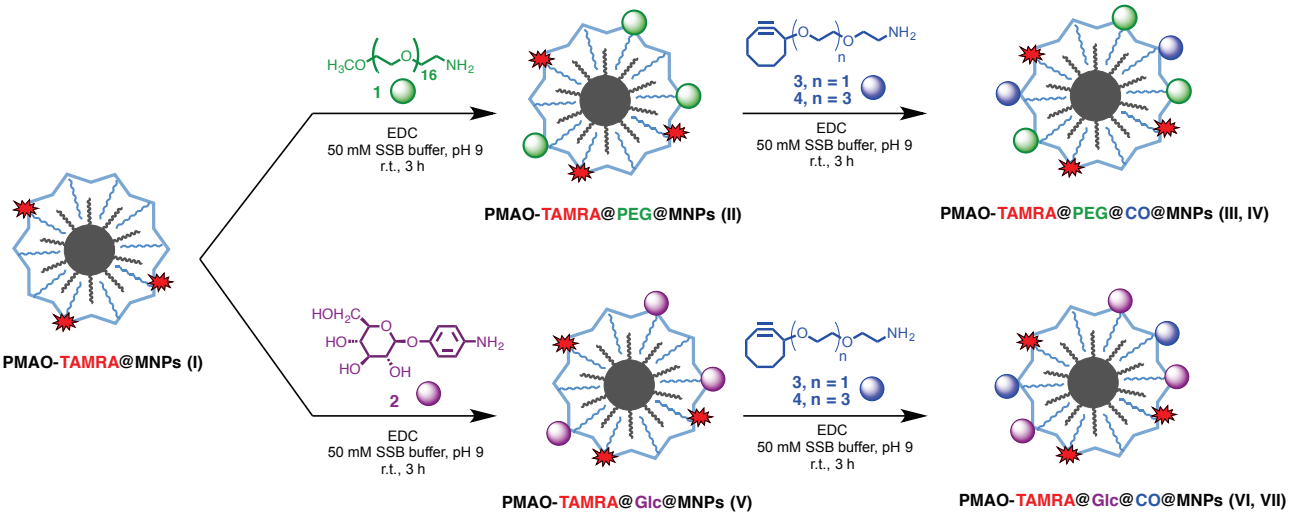

Scheme 2 Schematic synthetic approaches to obtain "clickable" magnetic nanoparticles

A possible explanation for this relatively low impact of SPAAC in the field of nano(bio)technology could be the fact that the synthesis of strained alkynes is usually a cumbersome and low-yield process.[10] Moreover, most cyclooctynes are hydrophobic; in fact, their hydrophilicity and reaction rate towards azides are usually inversely proportional.[27] This rather poor solubility in water can affect the colloidal stability of nanomaterials in biologically relevant media (aqueous buffers, cell culture media etc.). In fact, there are only few literature examples reporting the synthesis of cyclooctynyl derivatives with increased solubility in water for biofunctionalization of nanomaterials.[20,21]

Herein we report a simple functionalization protocol to obtain cyclooctyne-decorated, water-soluble magnetic nanoparticles (MNPs) suitable for SPAAC click chemistry. Our final aim is the SPAAC immobilisation of the cyclooctynyl-MNPs on living cell membranes labelled with azide groups for sub-lethal magnetic hyperthermia studies. For this purpose, the MNPs must have adequate colloidal stability in water and physiological media, which is achieved by incorporating short polyethylene glycol (PEG, **1**) or 4-aminophenyl β-D-glucopyranoside (Glc, **2**) moieties to their polymer coating. To overcome the problems associated with the poor water solubility of most strained alkynes, we propose the use of simple cyclooctynylamine derivatives (CO) bearing two short ethyleneglycol chains (**3** and **4**, Scheme 2). The incorporation of PEG, Glc and CO on the nanoparticles takes place using simple and straightforward amide coupling chemistry. As proof-of-concept demonstrating the availability of the cyclooctynyl moieties for SPAAC and thus the potential of the MNPs as SPAAC bioorthogonal probes, we immobilised the resulting "clickable" nanoparticles on silicon surfaces functionalised with azide groups. To the best of our knowledge, to the date there is no literature report on the use of SPAAC bioorthogonal click chemistry involving cyclooctynyl-functionalised MNPs. ‡

Results and discussion

Cyclooctynylamines **3** and **4** were easily prepared from 8,8-dibromobicyclo-[5.1.0]-octane)[21] following a three-step improved synthesis (Scheme 3, see ESI for experimental details and characterisation data). Ring-opening of the dibromocyclopropane with diethylene glycol or tetraethylene glycol in the presence of $AgBF_4$ afforded the corresponding intermediate alkoxylated (Z)-2-bromocyclooctenes, which were dehydrobrominated to cyclooctynes and simultaneously O-activated as nosyl esters using a mixture of 2-nosyl chloride and *t*-BuOK. Finally, each nosylate was reacted with ammonia in methanol to provide the amines **3** and **4** in approximately 40% overall yields avoiding using any chromatographic purification.

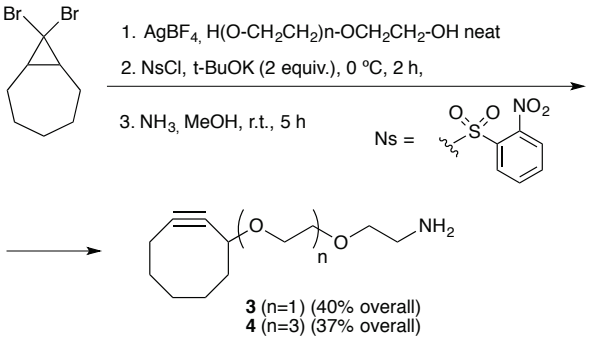

Scheme 3 Outline of the synthesis of cyclooctynylamine derivatives **3** and **4**

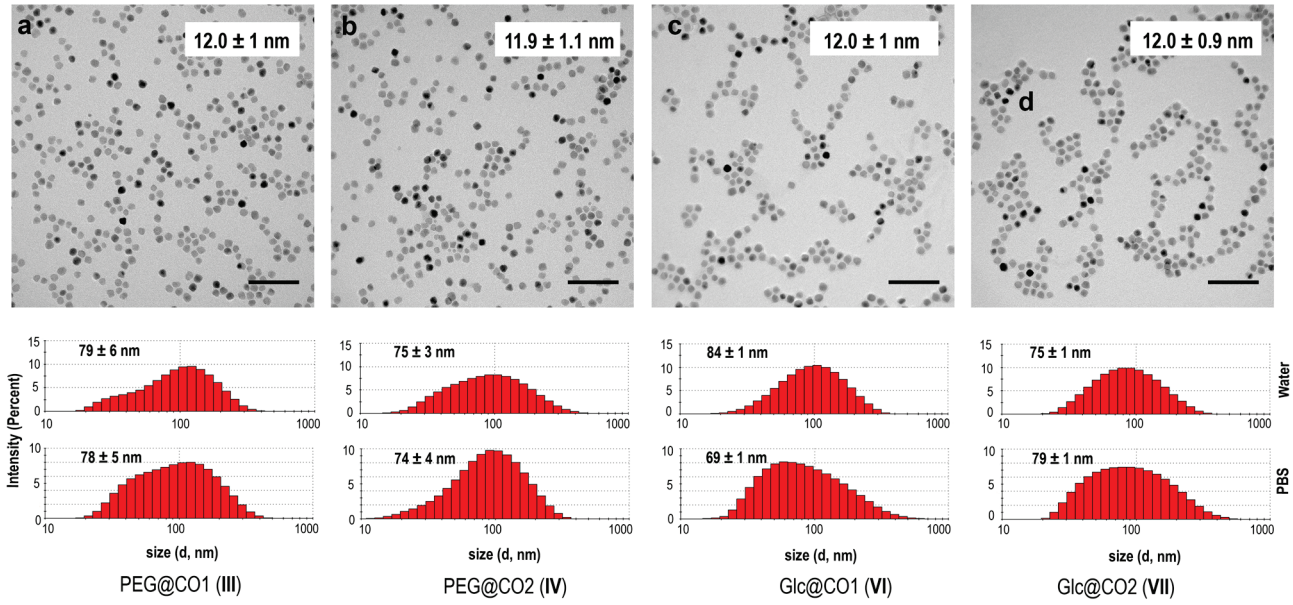

Figure 1 Top: TEM micrographs and core mean diameters determined from TEM. Bottom: hydrodynamic diameters (DLS size distribution histograms) of CO-functionalised MNPs in water and PBS suspensions. Scale bar for TEM images is 100 nm

The reactivity of the novel cyclooctynylamines towards copper-free "click" reactions with alkylazides was assessed for compound **4**. In a test reaction with benzylazide, monitored by Nuclear Magnetic Resonance (NMR) Spectroscopy at 40 °C in DMSO-*d6*, a total conversion was reached before 1 h at millimolar concentrations. A rate constant of k = 9.1 x 10^{-3} M was measured, in line with other functionalized cyclooctynes with similar structures (for details, see ESI).[27] Noteworthy, both cyclooctynes dispalyed excellent shelf life with no loss of stability or reactivity even after prolonged storage in aqueous solutions (up to 15 months).

Monodisperse spherical iron oxide nanoparticles stabilised with oleic acid ligands were synthesised in organic phase following a seed-mediated growth method, as previously described.[28,29] Briefly, 6-nm iron oxide nanoparticles were synthesised by thermal decomposition of iron acetylacetonate and used as "seeds" to grow NPs with an average diameter of 12 nm as determined from transmission electron microscopy (TEM) images (see Fig. S1). Subsequently, the hydrophobic MNPs were transferred to water using an amphiphilic polymer - poly(maleicanhydride-alt-1-octadecene) (PMAO) – using the protocol optimised by our group.[29,30] PMAO has hydrophobic aliphatic 18-carbon atoms chains that intercalate with the oleic acid chains on the surface of the MNPs and hydrophilic maleic anhydride moieties, which are exposed towards the outer surface of the polymer shell to provide stability in aqueous media. Moreover, upon basic hydrolysis each anhydride group can yield two carboxyl groups that can be used for further functionalization reactions. A fluorescent dye, tetramethylrhodamine 5- and 6-carboxamide cadaverine (TAMRA), was also incorporated to the polymer prior to the water transfer step in order to facilitate the observation of the MNPs by fluorescence microscopy.[30] For more details regarding the synthesis and water transfer of the MNPs, see ESI. As expected, TEM analysis of the water-soluble MNPs revealed no changes in the core diameter when compared to the hydrophobic ones (Fig. S2). The amount of polymer coating the NPs was estimated from the thermogravimetric analysis (TGA) of the sample and allowed to estimate a number of approximately 3900 COOH groups per MNP (see ESI for thermograms and calculation details).

To obtain the desired cyclooctynyl-decorated MNPs, a stepwise strategy (Scheme 2) was used. In the first step PMAO-MNPs **I** were decorated with PEG and Glc molecules, while in the second step the cyclooctynylamine derivatives **3** and **4** were incorporated.[§] For both steps, the amide coupling reaction between the carboxylic groups available on the MNP surface and the amine groups of the PEG, Glc and CO derivatives was used.

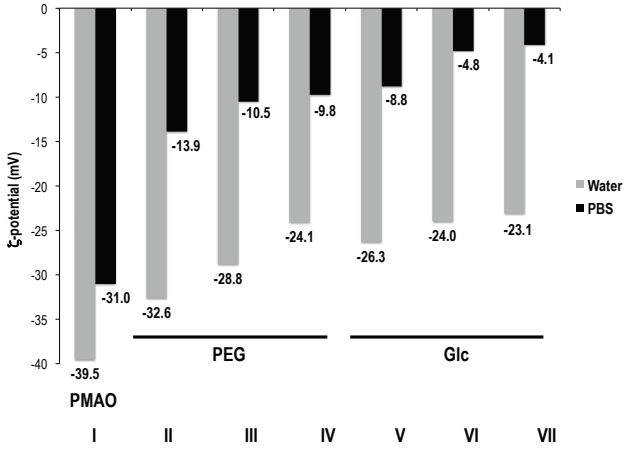

Figure 2 ζ-potential values of NPs II-VIII in water and PBS

The resulting functionalised MNPs **II**-**VII** were characterised by TEM, dynamic light scattering (DLS), ζ-potential measurements, agarose gel electrophoresis, infrared spectroscopy (FT-IR) and TGA analysis. TEM images revealed that the MNPs maintained the same Fe_3O_4 core diameter of approximately 12 nm upon successive functionalization steps (Figure 1; for TEM data of the intermediate NPs **II** and **V**, see ESI). Similar values for the mean hydrodynamic diameters of the four cyclooctynyl-MNPs were determined by DLS (see Figure 1; for full DLS data, see ESI Table S2), which is reasonable taking into account the small size of the molecules introduced onto the NP surface. Moreover, the cyclooctynyl-MNPs showed comparable hydrodynamic diameters in water and in phosphate buffered saline (PBS) suspensions. The success of each functionalization step was confirmed by ζ-potential measurements (Figure 2) and agarose gel electrophoresis (Fig. S6). A consistent decrease in the electrophoretic mobility of the MNPs after each functionalization was observed, corroborated with less negative ζ-potential values for NPs **II**-**VII** when compared to the starting PMAO-coated MNPs, which have a relatively high negative ζ-potential due to the presence of carboxyl groups on their surface. FT-IR spectroscopy (data not shown) further confirmed the successful incorporation of polyethyleneglycol and 4-aminophenyl β-D-glucopyranoside by the appearance of characteristic peaks for each molecule: 1092 cm^{-1} (asymmetric stretching CH_2-O-CH_2; PEG); 1509 cm^{-1} (aromatic C=C stretching; Glc) and 839 cm^{-1} (aromatic sp^2 C-H bending; Glc). Unfortunately, the presence of the cyclooctynylamine could not be confirmed by FT-IR spectroscopy due to the very low intensity of the C-C triple bond. Finally, from TGA analysis it was possible to estimate the number of molecules of PEG and Glc ligands per NP (see ESI for thermograms and detailed calculations). The TGA results indicate that approximately 25 % of the initial COOH groups were functionalised with PEG or Glc in the first step, corresponding to roughly 960 PEG molecules and 1000 Glc molecules per NP, respectively. Noteworthy, all cyclooctynyl-functionalised MNPs showed excellent colloidal stability both in PBS and complete Dulbecco´s Modified Eagle Medium (CDMEM) supplemented with 10% foetal bovine serum, indicating their suitability for future *in vitro* experiments. Figures S10-S12 show bright field microscope images of HTC 116 human colon carcinoma cells incubated with 100 μg/mL of cyclooctynyl-functionalised MNPs (**III**, **IV**, **VI** and **VII**) and with PMAO-coated MNPs (**I**) at three different time points: 5 min, 1 h and 24 h. While no signs of aggregation could be observed for cyclooctynyl-functionalised MNPs PMAO-coated MNPs **I** aggregated almost instantaneously, a similar behaviour being observed for the MNPs in suspension both in PBS and in CDMEM (Fig. S13).

The incorporation of the cyclooctynyl derivatives into the coating of the MNPs is not sufficient to guarantee that the MNPs will act as bioorthogonal probes. The cyclooctynyl fragments must maintain their reactivity and be presented onto the MNP surface in such a way that they are available for SPAAC reaction. Taking into account the small size of the alkynes **3** and **4**, the presence of the PEG chains on the surface of the MNPs **III** and **IV** could "mask" the cyclooctynyl moieties and prevent them from undergoing the SPAAC reaction. Thus, we have next interrogated the reactivity of the CO-decorated MNPs towards azides in order to obtain preliminary data for future *in vitro* studies. To this end, MNPs **II**-**VIII** were reacted with azide-functionalised silicon surfaces (Scheme 4).

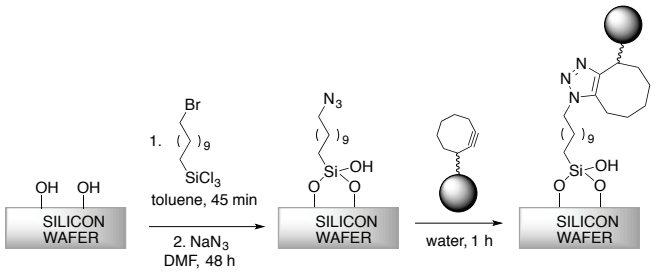

Scheme 4 Bioorthogonal strain-promoted "click" reaction of MNPs on surfaces

The surfaces were prepared by reacting piranha-activated silicon wafers stepwise with 11-bromoundecyltrichlorosilane and sodium azide.[31] The successful incorporation of the bromine and subsequent nucleophilic substitution by azide were verified using X-ray photoelectron spectroscopy (XPS) and static water contact angle measurements. In the high-resolution XPS spectrum of the sample containing bromine the peak at 70.49 eV could be clearly attributed to the 3d orbital of the bromine (see Fig. S14). Upon reaction with sodium azide the presence of a signature double peak in the N1s region (401-405 eV) of the XPS spectrum confirmed the successful incorporation of the azide functionality. The peak at lower binding energy (401.18 eV) corresponds to the two electron-rich outer nitrogen atoms of the azide, while the peak at 404.83 eV can be attributed to the central electron-deficient nitrogen atom; the relative intensity of these two peaks is 2:1, in accordance with literature data.[32,33] Water contact angle measurements also confirmed the success of each of the functionalization steps. Pristine silicon surfaces showed a contact angle of 57 º, which decreased significantly to 17 º after activation with piranha due to the pronounced hydrophilic character of the piranha-activated surface. After the incorporation of 11-bromoundecyltrichlorosilane the measured contact angle was of 90 º; further substitution of Br by N_3 showed a slight decrease in the value of the contact angle to 82 º.

The azide-functionalised surfaces were then incubated for 1h at room temperature with 125 mM aqueous solutions of MNPs **V**-**VIII** and of a commercially available DBCO derivative, DBCO-PEG_4-sulforhodamine B (see structure in Fig. S15). After extensive washing steps with water, acetone and ethanol the surfaces were submitted to SEM and XPS analysis. SEM images revealed the presence of nanoparticles only in the samples corresponding to the surfaces functionalised with azide groups and incubated with NPs bearing the cyclooctyne functionalities (Figure 3). This observation suggests that NPs are linked to the surface mainly through covalent bonds as a result of the SPAAC reaction, and not through adsorption. Indeed, the quantification of the surface coverage (in terms of percentage

of surface occupied by nanoparticles) revealed negligible values for the control experiments (less than 0.2% surface coverage both by PEG- and Glc-coated MNPs). Conversely, considerably higher percentages of surface coverage of up to 27% were found for the cyclooctynyl MNPs **III**, **IV**, **VI** and **VII** (see ESI for full details). In line with SEM observations, higher percentages of surface coverage were found for Glc-MNPs with respect to their PEG counterparts. Moreover, MNPs functionalised with the shorter cyclooctyne **3** showed higher surface coverage than the ones bearing the longer cyclooctyne **4**. These findings seem to suggest that a) the extent of functionalization with cyclooctynes is lower for the PEG-MNPs (probably due to steric hindrance induced by the PEG chains) and b) the longer cyclooctyne seems to have a lower availability for undergoing SPAAC reaction, perhaps due to the higher flexibility of the ethyleneglycol chain. As additional control experiments, both the piranha-activated and Br-functionalised silicon surfaces were also incubated with the same nanoparticle samples under similar experimental conditions to investigate possible non-specific adsorption events. As expected, a pronounced non-specific adsorption of all the NPs investigated was observed on the piranha-activated surfaces, due to its hydrophilicity, while a significantly lower density of nanoparticles could be appreciated in the SEM images corresponding to the Br-functionalised surfaces (see ESI for SEM images, Fig. S16 and S17). The XPS analysis of the azide-functionalised surface incubated with the dibenzocyclooctyne derivative clearly confirmed the formation of the triazole ring by the appearance of a new nitrogen peak at 399.96 eV and the decrease in the intensity of the nitrogen peaks corresponding to the azide (see Fig. S18). Moreover, an S2p peak at 163.13 eV could be identified, belonging to the dibenzylcyclooctyne-PEG4-5/6-Sulforhodamine B molecule. However, XPS could only confirm the presence of iron in the samples corresponding to the glucose-functionalised cyclooctynyl NPs (0.45 and 0.73 percentage atomic concentrations of Fe2p, respectively). This result can be explained by the higher surface coverage observed with the Glc NPs **VI** and **VII** when compared to their PEG counterparts.

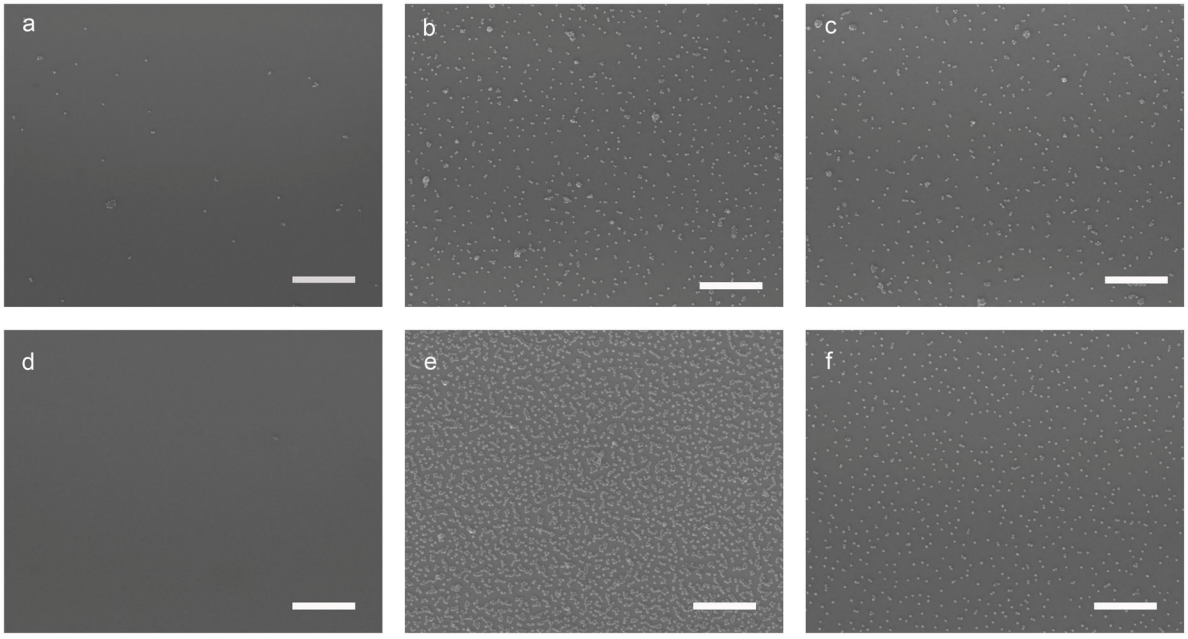

Figure 3 SEM micrographs of the azide-functionalised surfaces reacted with different MNPs. The percentage of surface coverage by MNPs is indicated between brackets for each nanoparticle type: a) PEG (**II**, 0.2); b) PEG@CO1 (**III**, 4.3); c) PEG@CO2 (**IV**, 2.9); d) Glc (**V**, 0); e) Glc@CO1 (**VI**, 27.1); f) Glc@CO2 (**VII**, 5.7). Scale bar is 500 nm

Conclusions

In this communication we present a simple functionalization strategy to obtain water-soluble magnetic nanoparticles suitable for bioorthogonal click chemistry reactions on surfaces. Using two simple hydrophilic cyclooctynylamine derivatives we prepared a small library of polyethylene glycol and glucose-functionalised "clickable" MNPs. These MNPs showed excellent colloidal stability in physiological media (PBS and cell culture medium) and were successfully immobilised on azide-functionalised silicon substrates, demonstrating their potential for strain-promoted bioorthogonal azide-alkyne cycloaddition. Moreover, we found that the reactivity of the MNPs towards azide surfaces depended on their surface functionality, which can dictate the availability of cyclooctynyl functional groups for SPAAC partners. We are currently investigating the incorporation of these MNPs on more complex substrates such as azide-modified lipid bilayers as simplified models of animal cell membranes. Studies regarding the cytotoxicity of the MNPs and their covalent attachment on living cell membranes are also underway. Importantly, the straightforward functionalization protocol reported here could be easily extended to the preparation of other types of

nanoparticles (quantum dots, gold NPs) suitable for bioorthogonal click chemistry applications.

Acknowledgements

This work was supported by Fondo Social de la DGA (grupos DGA), Ministerio de la Economía y Competitividad del Gobierno de España for the public funding of Proyectos I+D+I - Programa Estatal de Investigación, Desarrollo e Innovación Orientada a los Retos de la Sociedad (project n. SAF2014-54763-C2-2-R) and Gobierno Vasco (project IT-1033-16). R. M. F. also acknowledges financial support from Universidad de Zaragoza (JIUZ-2014-CIE-03) and European Union (Marie Skłodowska-Curie grant agreement No. 657215 OUTstandINg). The authors acknowledge the Laboratorio de Microscopias Avanzadas (LMA) at Instituto de Nanociencia de Aragon - Universidad de Zaragoza for offering access to their instruments and expertise. The authors would also like to thank Carlos Cuestas and Guillermo Antorrena (LMA) for helpful discussions.

Notes and references

‡ In an elegant approach to increase the sensitivity of magnetic resonance imaging (MRI) using MNPs, Gallo et al. reported the synthesis of "clickable" MNPs functionalised with complementary azides and strained alkynes.[34] *In vitro* and *in vivo*, these MNPs underwent SPAAC reaction, leading to T_2 signal enhancement due to clustering.

§ In the direct functionalization with the cyclooctynylamines **3** and **4** the PMAO-coated NPs showed rather poor colloidal stability, which resulted in aggregation during the reaction; to overcome this problem we pursued a stepwise functionalization strategy in which we introduced the PEG or glucose moiety in the first step to improve the stability of the NPs.

1 H. C. Kolb, M. G. Finn and K. B. Sharpless, *Angew. Chemie - Int. Ed.*, 2001, **40**, 2004–2021.
2 V. V. Rostovtsev, L. G. Green, V. V. Fokin and K. B. Sharpless, *Angew. Chem., Int. Ed. Engl.*, 2002, **41**, 2596–2599.
3 C. W. Tornøe, C. Christensen and M. Meldal, *J. Org. Chem.*, 2002, **67**, 3057–3064.
4 H. Nandivada, X. Jiang and J. Lahann, *Adv. Mater.*, 2007, **19**, 2197–2208.
5 J.-F. Lutz, *Angew. Chem. Int. Ed. Engl.*, 2007, **46**, 1018–25.
6 S. Kantheti, R. Narayan and K. V. Raju, *RSC Adv.*, 2015, **5**, 3687–3708.
7 X. Wang, B. Huang, X. Liu and P. Zhan, *Drug Discov. Today*, 2016, **21**, 118–132.
8 E. M. Sletten and C. R. Bertozzi, *Angew. Chem., Int. Ed. Engl.*, 2009, **48**, 6974–6998.
9 N. J. Agard, J. A. Prescher and C. R. Bertozzi, *J. Am. Chem. Soc.*, 2004, **126**, 15046–15047.
10 J. C. Jewett and C. R. Bertozzi, *Chem. Soc. Rev.*, 2010, **39**, 1272–9.
11 A. Borrmann and J. C. M. van Hest, *Chem. Sci.*, 2014, **5**, 2123.
12 E. Saxon and C. R. Bertozzi, *Science (80-.).*, 2000, **287**, 2007–2010.
13 N. J. Agard, J. M. Baskin, J. A. Prescher, A. Lo and C. R. Bertozzi, *ACS Chem. Biol.*, 2006, **1**, 644–648.
14 G. H. Hur, J. L. Meier, J. Baskin, J. A. Codelli, C. R. Bertozzi, M. A. Marahiel and M. D. Burkart, *Chem. Biol.*, 2009, **16**, 372–381.
15 W. Chen, J. M. Smeekens and R. Wu, *Chem. Sci.*, 2015, **6**, 4681–4689.
16 S. T. Laughlin, J. M. Baskin, S. L. Amacher and R. Carolyn, *Science (80-.).*, 2008, **320**, 664–667.
17 S. T. Laughlin and C. R. Bertozzi, *ACS Chem. Biol.*, 2009, **4**, 1068–1072.
18 J. M. Baskin, J. A. Prescher, S. T. Laughlin, N. J. Agard, P. V Chang, I. A. Miller, A. Lo, J. A. Codelli and C. R. Bertozzi, *Proc. Natl. Acad. Sci. U. S. A.*, 2007, **104**, 16793–7.
19 H. E. Bostic, M. D. Smith, A. A. Poloukhtine, V. V. Popik and M. D. Best, *Chem. Commun.*, 2012, **48**, 1431–1433.
20 E. Lallana, E. Fernandez-Megia and R. Riguera, *J. Am. Chem. Soc.*, 2009, **131**, 5748–5750.
21 A. Bernardin, L. Guyon, P. Delannoy, D. Bonnaffe and I. Texier, *Bioconjugate Chem.*, 2010, **21**, 583–588.
22 H. Koo, S. Lee, J. H. Na, S. H. Kim, S. K. Hahn, K. Choi, I. C. Kwon, S. Y. Jeong and K. Kim, *Angew. Chemie - Int. Ed.*, 2012, **51**, 11836–11840.
23 S. Lee, H. Koo, J. H. Na, S. J. Han, S. Y. Min, Jeong, I. C. Kwon, K. Choi, K. Kim and L. E. E. E. T. Al, *ACS Nano*, 2014, **8**, 2048–2063.
24 S. B. Lee, H. L. Kim, H. J. Jeong, S. T. Lim, M. H. Sohn and D. W. Kim, *Angew. Chemie - Int. Ed.*, 2013, **52**, 10549–10552.
25 P. Gobbo, S. Novoa, M. C. Biesinger and M. S. Workentin, *Chem. Commun. (Camb).*, 2013, **49**, 3982–4.
26 P. Gobbo, Z. Mossman, A. Nazemi, A. Niaux, M. C. Biesinger, E. R. Gillies and M. S. Workentin, *J. Mater. Chem. B*, 2014, **2**, 1764.
27 M. F. Debets, J. C. M. van Hest and F. P. J. T. Rutjes, *Org. Biomol. Chem.*, 2013, **11**, 6439–55.
28 S. Sun, H. Zeng and D. Robinson, *J. Am. Chem. Soc.*, 2004, **126**, 273–279.
29 M. Moros, B. Pelaz, P. López-Larrubia, M. L. García-Martin, V. Grazú and J. M. de la Fuente, *Nanoscale*, 2010, **2**, 1746–55.
30 M. Moros, B. Hernáez, E. Garet, J. T. Dias, B. Sáez, V. Grazú, Á. González-Fernández, C. Alonso and J. M. de la Fuente, *ACS Nano*, 2012, **6**, 1565–1577.
31 T. Lummerstorfer and H. Hoffmann, *J. Phys. Chem. B*, 2004, **108**, 3963–3966.
32 H. Mizuno and J. M. Buriak, *ACS Appl. Mater. Interfaces*, 2010, **2**, 2301–2307.
33 M. S. Azam, S. L. Fenwick and J. M. Gibbs-Davis, *Langmuir*, 2011, **27**, 741–750.
34 J. Gallo, N. Kamaly, I. Lavdas, E. Stevens, Q. De Nguyen, M. Wylezinska-Arridge, E. O. Aboagye and N. J. Long, *Angew. Chemie - Int. Ed.*, 2014, **53**, 9550–9554.